Catalysis Today 175 (2011) 256–263

Contents lists available at ScienceDirect

Catalysis Today

journal homepage: www.elsevier.com/locate/cattod

Photocatalytic reduction of CO_2 to hydrocarbons using $AgBr/TiO_2$ nanocomposites under visible light

Mudar Abou Asi[a], Chun He[a,b,*], Minhua Su[a], Dehua Xia[a], Long Lin[a], Huiqi Deng[a], Ya Xiong[a,b], Rongliang Qiu[a,b], Xiang-zhong Li[c]

[a] *School of Environmental Science and Engineering, Sun Yat-sen University, Guangzhou 510275, China*
[b] *Guangdong Provincial Key Laboratory of Environmental Pollution Control and Remediation Technology, Guangzhou 510275, China*
[c] *Department of Civil and Structural Engineering, The Hong Kong Polytechnic University, Hong Kong, China*

ARTICLE INFO

Article history:
Received 14 October 2010
Received in revised form 31 January 2011
Accepted 28 February 2011
Available online 2 April 2011

Keywords:
CO_2 reduction
Photocatalyst
$AgBr/TiO_2$
Visible light

ABSTRACT

Urgent development of effective and low-cost technologies for reduction CO_2 is needed to address global warming caused by atmospheric CO_2 and the depletion of fossil fuels. In this investigation, an effective photocatalytic reduction of CO_2 using $AgBr/TiO_2$ photocatalyst under visible light ($\lambda > 420$ nm) was studied. The nanostructured $AgBr/TiO_2$ photocatalyst was prepared by the deposition-precipitation method in the presence of cetyltrimethylammonium bromide (CTAB), and characterized by X-ray diffraction (XRD), diffuse reflectance spectra (DRS), scanning electron microscopy (SEM) and transmission electron microscopy (TEM). Their photocatalytic activities were evaluated by the reduction yield in the presence of CO_2 and water. The experiment results showed that 23.2% $AgBr/TiO_2$ had relatively high reduction yields under visible-light irradiation for 5 h, with a methane yield of 128.56, methanol yield of 77.87, ethanol yield of 13.28, and CO yield of 32.14 μmol g^{-1}, respectively. The highly efficiently photocatalytic activities of $AgBr/TiO_2$ in the reduction process of CO_2 is attributed to its strong absorption in the visible-light region. In addition, it was found that $AgBr/TiO_2$ photocatalyst was stable in the repeated uses under visible light irradiation, due to the transfer of photoexcited electrons from the conduction band of well-dispersed AgBr to that of TiO_2.

1. Introduction

Global warming caused by large-scale emission of atmospheric CO_2 and the depletion of fossil fuels are two critical addressing problems in the near future [1,2]. The reduction of CO_2 into the useful compound has been regarded as an important research area for solving both problems [3]. One of promising research studies focusing on the economic photocatalytic reduction of CO_2 to form products of interest were carried out using various semiconductor catalysts in a heterogeneous system [4–6]. Among the applied photocatalysts, titania has been considered the most appropriate candidate for photocatalyic process since its conduction band energy ($E_{cb} \approx -0.5$ eV vs. NHE at pH 7) is comparable to the reduction potentials of CO_2 (e.g., the later is -0.24 V vs. NHE for reduction of CO_2 to CH_4, and -0.38 V vs. NHE for reduction of CO_2 to methanol in aqueous solution at pH 7) [6,7]. Yet, it has so far yielded low carbon dioxide conversion rates despite using UV irradiation for band gap excitation [6,8].

There have been a few previous works done on how the modified titanium obtains visible-light utilization efficiency to act as visible-light active photocatalysts for CO_2 reduction. These works include (1) doping TiO_2 with transition metal [5,6], (2) doping TiO_2 with nonmetal atoms [9,10], and (3) sensitizing dye molecules on the surface of TiO_2 [11]. However, it is still a challenge to explore the highly efficient modified titania for the reduction of CO_2 under visible light, due to the instability of the metal-doped titania, relatively low absorption coefficiency of the nonmetal-doped titania in the visible light region, and toxicity and self-photodegradation of the organic sensitizer [12,13]. One of the promising approaches to overcome this disadvantage is to modify TiO_2 with a narrow band gap semiconductor which is functioned in the visible light region [8]. In this process, the photogenerated electrons from the conduction band of the narrow band gap semiconductor excited by visible light could be injected into the conduction bands of TiO_2, resulting in the enhanced visible light activity [14].

Recently, modifying titania by colorful inorganic materials received much attention because of their stability and relatively strong absorption in the visible light region [12–15]. The silver

---

[*] Corresponding author at: School of Environmental Science and Engineering, Sun Yat-sen University, Guangzhou 510275, China. Tel.: +86 20 80958871; fax: +86 20 39332690.
E-mail address: hechun@mail.sysu.edu.cn (C. He).

0920-5861/$ – see front matter © 2011 Elsevier B.V. All rights reserved.
doi:10.1016/j.cattod.2011.02.055

bromide (AgBr) is well-known as photosensitive materials with a direct band gap of 4.29 eV (289 nm) and an indirect band gap of 2.64 eV (470 nm) [12,16,17], which can be applied in photocatalytic reaction by coupling some supporting materials [12,13,18–20]. In the photosensitive process, AgBr absorbs a photon and generates an electron and a positive hole. If the photographic process (i.e. interstitial ions combined with electrons to form silver atoms) is inhibited, the generated electron and hole can be used in the photocatalytic process [12,14]. It has been found that AgBr can maintain its stability and enhance the catalytic activity after AgBr is coupled with TiO_2 [13,14], alumina [18,19], zeolite [20] etc. In our previous work, we also found that AgBr supported by cetyltrimethylammonium bromide can maintain its stability [21]. Therefore, AgBr coupled with some supporting material could be effective in photocatalytic reaction and maintain its stability under irradiation. But till now, most pioneering publications of AgBr photocatalytic activity were related to the oxidation reactions for the degradation of azodyes and organic pollutants [12], decomposition of CH_3CHO [20], and destruction of bacteria etc. [13], only few reports were subjected to the photocatalytic reduction of NO_x using silver halide/Al_2O_3 [19,22].

Considering the reduction of CO_2 is an electron-consuming process [3,5,8], the injected electrons on the supporting material from conduction band of AgBr would be scavenged by CO_2, which could promote the photostability of AgBr by prohibiting the interstitial silver ions to silver atoms. Thus, we are encouraged to employ AgBr nanocomposites supported on TiO_2 to investigate their photocatalytic performance for the reduction of CO_2 under visible light. In this study, we will report our preliminary results of an effective photocatalytic reduction of CO_2 under visible light ($\lambda > 420$ nm) using AgBr/TiO_2 photocatalyst in which AgBr was well dispersed on TiO_2, and investigate the feasibibily and the mechanism of AgBr/TiO_2 with a highly efficient performance of photocatalytic reduction of CO_2 to hydrocarbons under visible light.

2. Experimental

2.1. Materials

TiO_2 (Degussa P25) powder with an average particle size of 30 nm and surface area of 50 $m^2\,g^{-1}$ was purchased from Degussa AG Company as a regular TiO_2 catalyst. CO_2 gas (99.99%) was obtained from Foshan Ruike Gas Co., Ltd. in China. Cetyltrimethylammonium bromide (CTAB, $C_{16}H_{33}N^+(CH_3)_3Br^-$; purity: >98%) was purchased from Tianjing Fuchen Chemical Reagent Co., Ltd. in China. $AgNO_3$ with analytical grade was purchased from Guangdong Guanhua Chemical Co., Ltd. in China. Other chemicals with analytical grade were obtained as reagents and used without further purification. Deionized water was used throughout this study.

2.2. Preparation of AgBr/TiO_2 catalyst

AgBr/TiO_2 was prepared by the deposition-precipitation method in the presence of cation surfactant of CTAB [13]. An appropriate amount of TiO_2 (P25) based on TiO_2 content in the sample was added to 100 mL of CTAB aqueous solution with a concentration of 0.01 M (10 times above the CMC of CTAB 9.8×10^{-4} M) [21], and the suspension was sonicated for 30 min and then stirred magnetically for 30 min. Then 0.0012 mol of $AgNO_3$ in 2.3 mL of amomonia hydroxide (25 wt.% NH_3) was quickly added to the suspension. In this process, cationic surfactant CTAB was adsorbed onto the surface of TiO_2 at alkaline condition to limit the number of nucleation sites for the formation of AgBr aggregates, leading to well-dispersed AgBr on TiO_2 support. In addition, the amount of bromide ion from CTAB is more than sufficient to precipitate Ag^+ from the added $AgNO_3$ in aqueous solution. The resulting mixture was stirred at room temperature for 12 h. The product was filtered, washed with deionized water, dried at 75 °C, and subsequently sintered in a muffle furnace at different temperatures (200, 400, 500 and 700 °C) for 3 h. A series of AgBr/TiO_2 was prepared with the AgBr content in the sample was at 7.0, 11.6, 23.2, 46.4 and 175.0% (wt.AgBr/wt.TiO_2), respectively, by changing the amount of TiO_2 in the suspension solution.

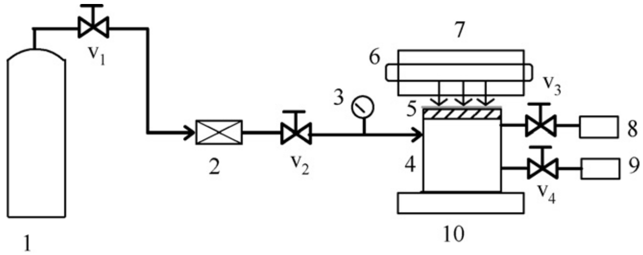

Fig. 1. Schematic diagram of photocatalytic reduction system: 1, CO_2 gas cylinder; 2, flow meter; 3, pressure digital meter; 4, stainless steel vessel; 5, O-ring glass window; 6, Xe lamp; 7, cooling system; 8, gas sampling; 9, liquid sampling; 10, magnetic stirrer; V_1, V_2, V_3, and V_4 are valves.

2.3. Characterization of AgBr/TiO_2 catalyst

The prepared AgBr/TiO_2 powders were first analyzed by X-ray diffraction (XRD) method using a diffractometer (Bruker AXS, Germany) with radiation of Cu target (K_α, λ = 1.54059 Å). Scanning electron microscopy (SEM) images were obtained with a JSM-6330F field emission scanning electron microscope (JEOL, Japan) using an acceleration voltage of 20 kV. The content of AgBr in the catalyst was determined by SEM-EDS-EBSD thermal field emission scanning electron microscopy (JEOL, Japan). The AgBr/TiO_2 powders were then examined by a transmission electron microscope (TEM, JEM-2010HR). X-ray photoelectron spectroscopy (XPS) data was recorded with the AlKα line at 100 W using a Perkin-Elmer PHI-5600ci. The catalysts were further examined by a spectrophotometer (Shimadzu UV-PC3101PC) with an integrating sphere (Specular Reflectance ATT.5DEG) to record their diffuse reflectance spectra (DRS), in which a baseline was corrected by using a calibrated sample of barium sulfate. Zeta potential measurements were performed using a ZetaPALS analyzer (Brookhaven, USA).

2.4. Photocatalytic CO_2 reduction experiments

Photocatalysis reduction was carried out in a stainless steel vessel with valves for evacuation and gas feeding as shown in Fig. 1, in which an O-ring sealed glass window was placed at the top for admitting light irradiation. A 150 W Xe lamp (Shanghai Aojia Lighting Appliance Co., Ltd.) with UV cutoff filter (providing visible light with $\lambda > 420$ nm) was used for irradiation. In a typical batch, 0.5 g of prepared AgBr/TiO_2 powder was suspended in 100 ml of 0.2 M $KHCO_3$ solution in the vessel. The pH value was adjusted by NaOH and HCl to the definite values before the experiment and not controlled during the reaction. Prior to the irradiation, pure CO_2 (99.99%), via a flow controller, was passed through the solution for 30 min to remove the oxygen, and then closed maintaining a pressure of 7.5 MPa inside the reactor. During reaction, the powders were continuously agitated to prevent the sedimentation of the catalyst by a magnetic stirrer, and the photocatalytic reaction lasted for 5 h at room temperature. After illumination, small aliquots of the suspension were withdrawn by syringe, filtered through Millipore membranes, and then analyzed. Gas samples were performed with a gas-tight syringe through a septum. Reaction products in liquid phase were analyzed using a gas chromatograph (Agilent HP6890N)

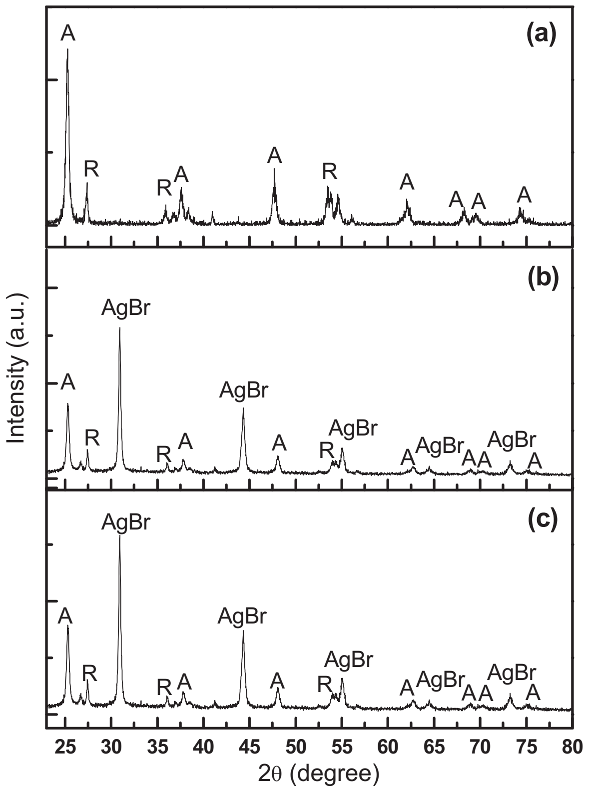

Fig. 2. XRD pattern of (a) TiO_2, (b) fresh 23.2% $AgBr/TiO_2$, and (c) used 23.2% $AgBr/TiO_2$ after 5 h visible light irradiation (A: anatase, and B: rutile).

equipped with a flame ionization detector (FID) and a HP-5 capillary column (30 m × 320 μm × 0.50 mm). The product in gas phase was analyzed by GC/MS Hewlett-Packard (HP) 6890 gas chromatography with a HP 5973 mass detector. A 60 m length × 0.32 mm I.D. 1.8 m film thickness HP-VOC column (Agilent Scientific, USA) was used. The oven was programmed as following rates, the initial temperature of the column was 40 °C hold for 2 min, followed by a ramp of 5 °C min^{-1} to 120 °C (1 min hold), injection model splitless, for 1 μL sample.

3. Results and discussion

3.1. Characterization of $AgBr/TiO_2$

The prepared fresh $AgBr/TiO_2$ was first examined by XRD as shown in Fig. 2a. The XRD results showed that both anatase and rutile were present in the $AgBr/TiO_2$ catalyst. In the meantime, the crystalline AgBr was found in the fresh $AgBr/TiO_2$ at around $2\theta = 26.7°$, 30.9°, 44.3°, and 55.0° (Fig. 2b), indicating a hexagonal structure for the synthesized AgBr according to the report by Rodrigues and Uma et al. [20]. No XRD peaks attributed to metallic Ag were observed in the spectrum of $AgBr/TiO_2$. In our synthesis process, the metallic Ag was not observed, and all of the silver species can be precipitated and deposed by CTAB. In addition, we found that the XRD pattern of used $AgBr/TiO_2$ after 5 h visible-light irradiation with a 150 W Xe lamp (Fig. 2c) was almost the same as that of fresh $AgBr/TiO_2$, no diffraction peaks assigned to metallic Ag (38.2°, 44.4°, 64.4° and 77.4°) [23] were detected in the used $AgBr/TiO_2$ sample. XRD results indicated that AgBr maintained stable after 5 h visible-light irradiation.

The used $AgBr/TiO_2$ was further characterized by XPS measurement. Fig. 3 presents XPS spectrum of Ag3*d* region and Br 3*d* region for used $AgBr/TiO_2$ after 5 h irradiation. Two peaks from Ag $3d_{5/2}$ and $3d_{3/2}$ were observed at 369.5 eV and 375.5 eV. Because the Ag3*d* photoelectron peaks are relatively insensitive to oxidation state changes, it is impossible to distinguish between Ag(0) metal and Ag(I) [24]. However, an Auger parameter analysis using the Ag MNV Auger peak at 1140.0 eV on the binding energy scale clearly indicates that the Ag is in a mono-valent state [24]. XPS ananlysis indicated that AgBr maintained stable after 5 h visible-light irradiation.

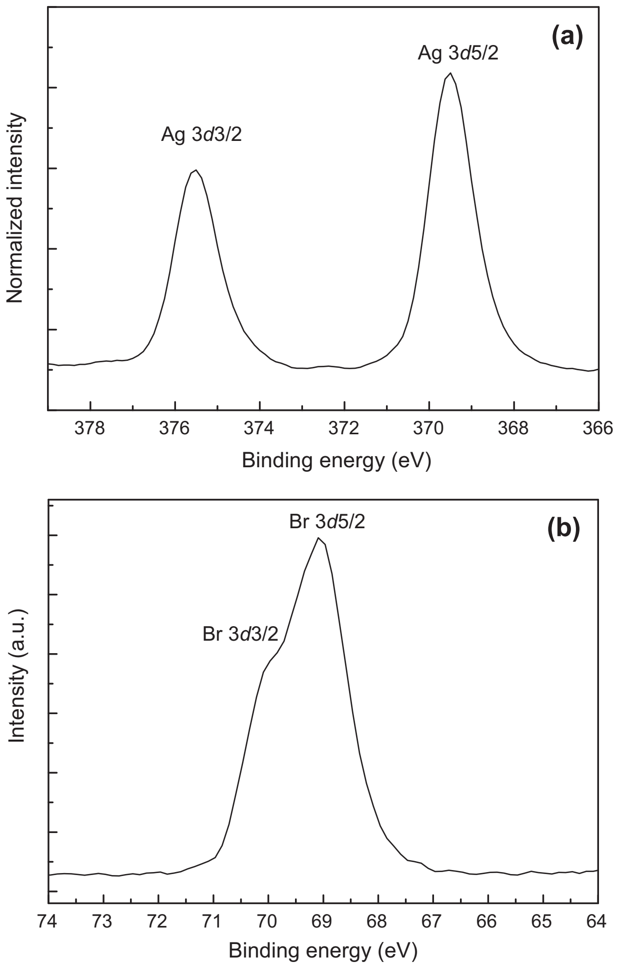

Fig. 3. XPS peaks of (a) Ag 3*d* peaks, and (b) Br 3*d* for used $AgBr/TiO_2$ after 5 h irradiation.

According to earlier studies, we noticed that irradiation led to the coexistence of AgBr and metallic Ag by the combination of interstitial ions with electrons [13,14], although there are some reports related to photostability without any formation of Ag for $AgCl/TiO_2$ [15] and AgI/TiO_2 [12] photocatalyst as well. For example, 1.2 wt.% Ag was formed after 14 h irradiation in $AgBr/TiO_2$ [14], which is different from our results of no metalic Ag. This might be ascribed to the difference of photocatalytic reduction process by consuming electron in our present study. In addition, recently, Zang et al. reported that dispersing AgBr on TiO_2 to form smaller particles might inhibit the formation of larger cluster and delay AgBr decomposition [14]. Therefore, AgBr with a small size would be stabilized by the surrounding support of TiO_2 while $AgBr/TiO_2$ was applied in the photocatalytic reduction of CO_2. However, further experiment is necessary to elucidate the stability of $AgBr/TiO_2$.

The $AgBr/TiO_2$ catalysts before irraditation were examined by SEM as showed in Fig. 4a. It can be seen from that the prepared fresh $AgBr/TiO_2$ was spherical particles and the particle size was relatively uniform around 50 μm. Although the SEM results did

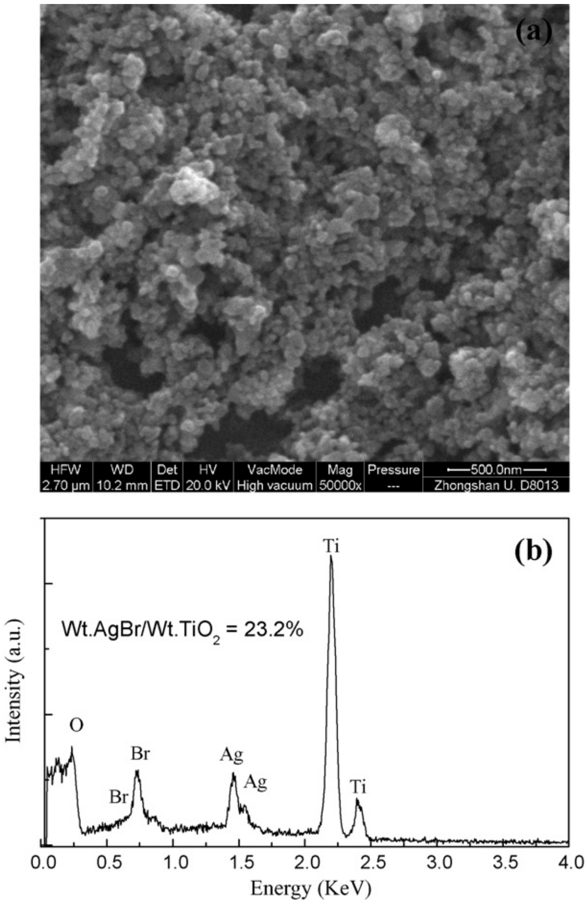

Fig. 4. (a) SEM image, and (b) EDS spectrum of 23.2% $AgBr/TiO_2$ before irradiation.

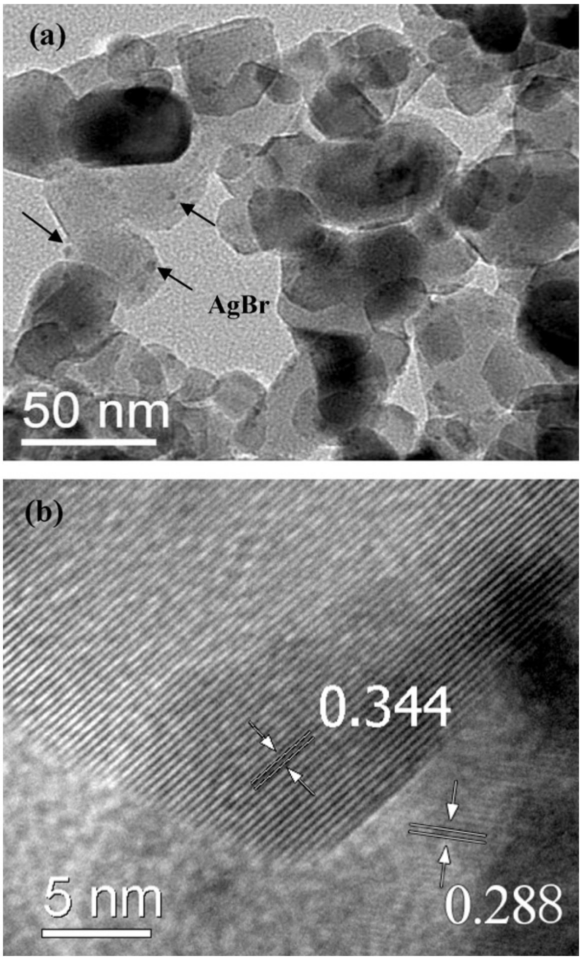

Fig. 5. (a) TEM image of $AgBr/TiO_2$, and (b) HRTEM image of $AgBr/TiO_2$.

not provide clear information about the size distribution of AgBr on TiO_2 particulates, EDS analysis of AgBr in $AgBr/TiO_2$ demonstrated that AgBr was uniformly dispersed on TiO_2 surface (Fig. 4b). The mass ratio of AgBr:TiO_2 obtained in the powder was almost closed to the theoretical calculated value of $AgBr/TiO_2$, for example, $AgBr/TiO_2$ with calculated value of 22.0% AgBr content was determined to be 23.2%.

Fig. 5 showed TEM images of $AgBr/TiO_2$. It can be seen that AgBr nanoparticles (black image) with a size of c.a. 5 nm contacted with TiO_2 nanoparticles (Fig. 5a), indicating that AgBr nanoparticles were well dispersed on the surface of TiO_2 nanoparticles. To further obtain the structure information on the interface of TiO_2 and AgBr nanoparticle, the interface of TiO_2 and AgBr nanoparticle was charaterized by HRTEM (Fig. 5b). The interplanar spacing on TiO_2 (0.344 nm) corresponded to the (1 0 1) planes of anatase, while the interplanar spacing on AgBr (0.288 nm) corresponded to the (2 0 0) planes of AgBr, further confirming the contact between the interface of TiO_2 and AgBr nanoparticles. Such a direct contact between the two particles would be crucial for improving the photocatalytic activity of the catalyst.

Considering the excellent photosensitive performance of AgBr, $AgBr/TiO_2$ catalysts were analyzed by UV–vis absorption spectra in the wavelength range of 250–800 nm and the absorption spectra of TiO_2 and $AgBr/TiO_2$ catalysts were shown in Fig. 6. It can be seen that $AgBr/TiO_2$ shows an absorption edge at 432 nm. The absorption was attributed to the contribution of AgBr since TiO_2 has no absorption at around this wavelength (Fig. 6a). Compared to TiO_2 catalysts, all $AgBr/TiO_2$ catalysts had a substantial red shifting of the absorption edge due to dispersed AgBr as well as a better optical absorption generally in the visible region of 400–700 nm with the increasing amounts of AgBr. The plot of the transformed Kubelka-Munch function versus the energy of light illustrates a bandgap of 2.9 eV (432 nm) for 23.2% $AgBr/TiO_2$ (Fig. 6b). In addition, a broad significant absorption shoulder occurred in the region of 450–700 nm corresponding to the indirect band gap of AgBr [12], consequently, $AgBr/TiO_2$ is sensitive to the whole visible light region. Thus, it is believed that the extension of light absorbance of $AgBr/TiO_2$ is an essential condition and would be beneficial to conduct photocatalytic reduction of CO_2 with water to hydrocarbon under visible light irradiation.

3.2. Photocatalytic reduction activity of $AgBr/TiO_2$

The photocatalytic reaction activity of prepared photocatalysts was evaluated by reduction of CO_2 with water under the visible light irradiation for 5 h. The gas chromatograph graphs of the photocatalytic products on the prepared $AgBr/TiO_2$ predominated showed the formation of methane and CO in gas phase, methanol and ethanol in liquid phase. Other products such as formic acid, formaldehyde and hydrogen were not detectable in our GC analysis. In contrast, these products (methanol, ethanol, methane and CO) were neither detected in the dark nor without the presence of photocatalysts, indicating that the presence of both the visible-light irradiation and photocatalyst are indispensable for the photocatalytic reduction of CO_2 with water.

Fig. 7a shows the effect of AgBr content on the yield of photocatalytic product using TiO_2 and prepared $AgBr/TiO_2$ under visible-light irradiation. It can be seen that the product yield is

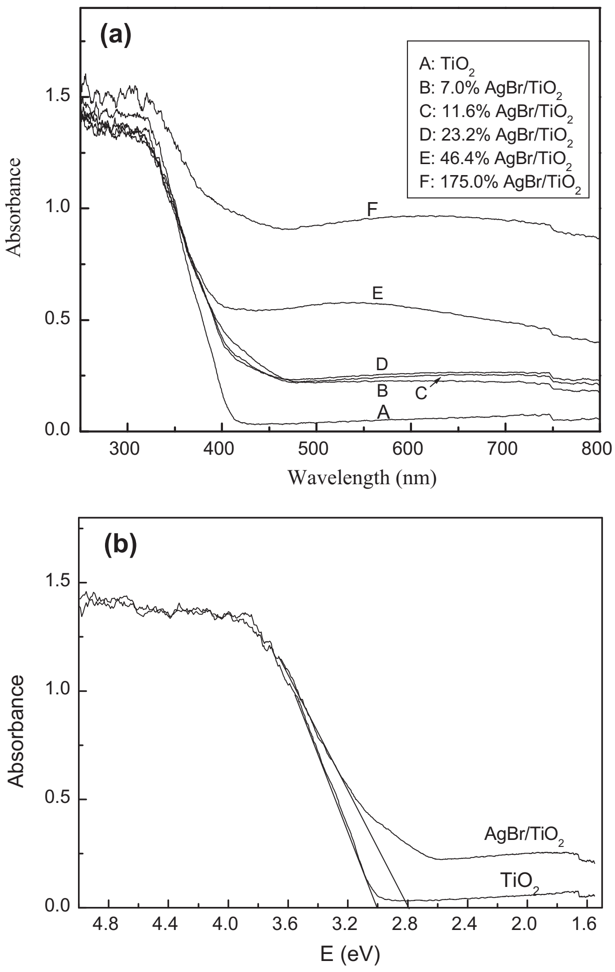

Fig. 6. UV–vis diffuse reflectance spectra of photocatalysts: (a) absorbance vs. light-absorbed wavelength, (b) Kubelka-Munch function vs. light-absorbed energy.

dependent on the content of AgBr. In a batch reaction, the product yield increased with the increase of AgBr content, then decreased as AgBr content exceeded 23.2%. The maximum yield of methane, methanol, ethanol, and CO using 23.2% $AgBr/TiO_2$ under visible light for 5 h reached 128.56, 77.87, 13.28, and 32.14 $\mu mol\,g^{-1}$, respectively. In this study, the experimental results showed that the photocatalytic reduction activity of $AgBr/TiO_2$ with AgBr content up to 23.2% achieved an effective performance. Evidently, the presence of AgBr plays an important role and can increase the photocatalytic yields of hydrocarbon under visible-light irradiation. However, the excessive AgBr dispersed on the TiO_2 will lead to the aggregation of AgBr, the photogenerated electrons are difficult to be transferred to that of TiO_2, consequently leading to a relatively lower activity. Therefore, an appropriate ratio of AgBr to TiO_2 can greatly improve the visible-light activity of catalyst.

The experimental results in Fig. 7b demonstrate that the calcination temperature also slightly affects the photocatalytic yield of hydrocarbon. It seems that the $AgBr/TiO_2$ prepared at 500 °C achieved the highest yield of hydrocarbon in the reduction of CO_2 due to the good crystallization during the calcination process. It is believed that the high calcination temperature of 700 °C resulted in large particles due to the aggregation of nanoparticles, which could reasonably explain the decreased yield of hydrocarbon.

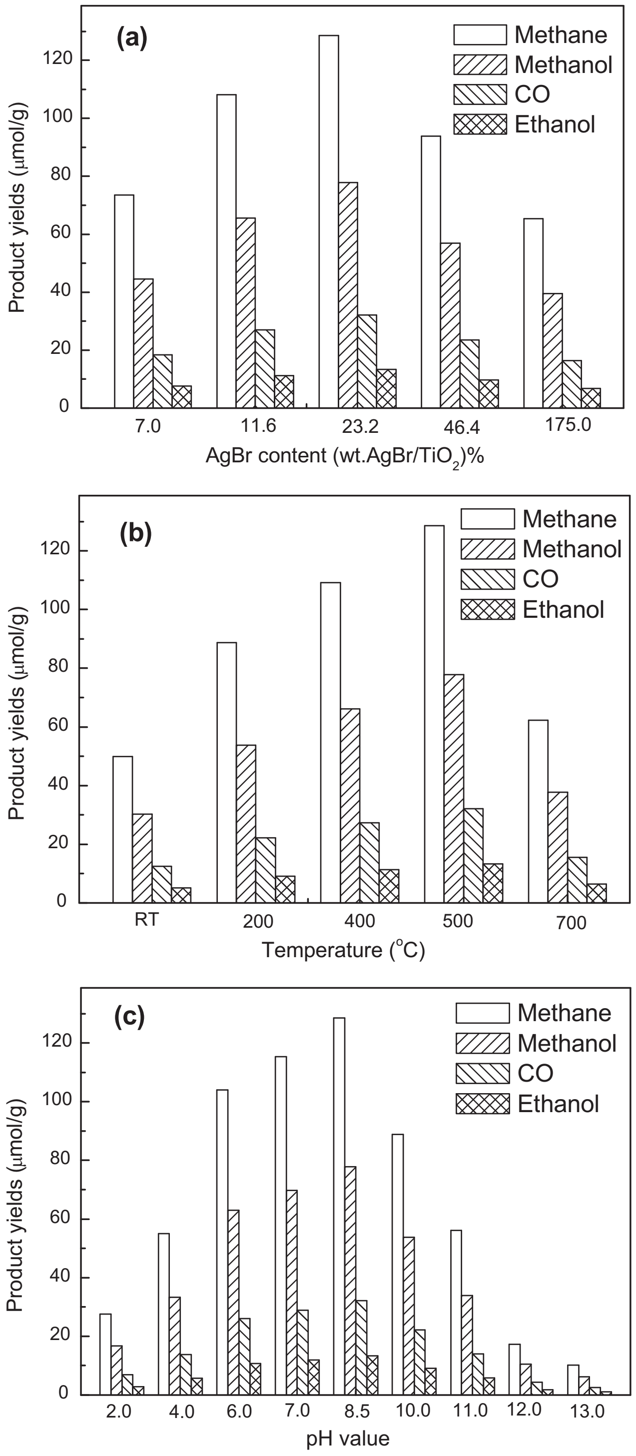

Fig. 7. Yield of photocatalytic products under 5 h visible light irradiation on (a) AgBr content using $AgBr/TiO_2$ sintered at 500 °C in pH 8.5 aqueous media, (b) calcination temperature using 23.2% $AgBr/TiO_2$ in pH 8.5 aqueous media, and (c) pH value using 23.2% $AgBr/TiO_2$ sintered at 500 °C.

The photoreduction process of CO_2 involved H· radicals and carbon dioxide anion radicals formed by electron transfer from the conduction band [3,9,10], therefore, the pH value was crucial in the photoreduction of CO_2. Fig. 7c showed the effect of pH value on the yield of photocatalytic products on $AgBr/TiO_2$. It was found that the product yield increased with the pH value to 8.5, and then decreased upon the further increase in the pH value. Obviously, the neutral and weak alkaline pH value is beneficial to the photoreduction of CO_2. This can be explained by the following reasons: (1) The OH^- ions in aqueous solution could act as strong hole-scavengers and reduce the recombination of hole-electron pairs [9,25,26], beneficial to facilitate the reduction of CO_2. In contrast,

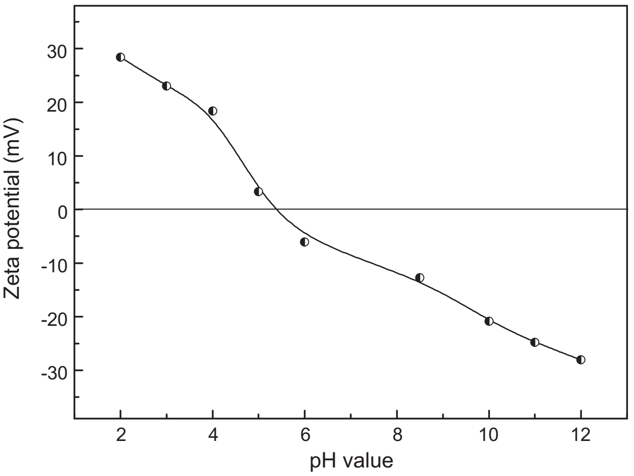

Fig. 8. Zeta potential for suspension of $AgBr/TiO_2$ nanoparticles in the presence of 0.2 M $KHCO_3$ solution.

H^+ in aqueous solution could be involved in the electron competition with CO_2 reduction (i.e. $H^+ + e^- \rightarrow H\cdot$), leading to the less yields of hydrocarbons. (2) More CO_2 can be dissolved in basic solution to form HCO_3^- ions (i.e. $CO_2 + OH^- \rightarrow HCO_3^-$) than pure water or acidic solution [27], resulting in a higher yields of hydrocarbons in the photoreduction process. (3) The neutral and weak alkaline pH value is beneficial to the adsorption of CO_2 on the catalyst from the zeta potential result of $AgBr/TiO_2$ (Fig. 8). It can be seen that the electrostatic force existed between CO_2 and the catalyst due to positively charged catalyst at pH < 5.4, while the electrostatic repulsive force existed between CO_2 and the catalyst due to negatively charged at pH > 5.4. Therefore, a relatively higher photocatalytic reduction activity was achieved in the neutral and weak alkaline pH range, representing the overall combined effect of the higher concentration of OH^- ions but lower electrostatic repulsive force.

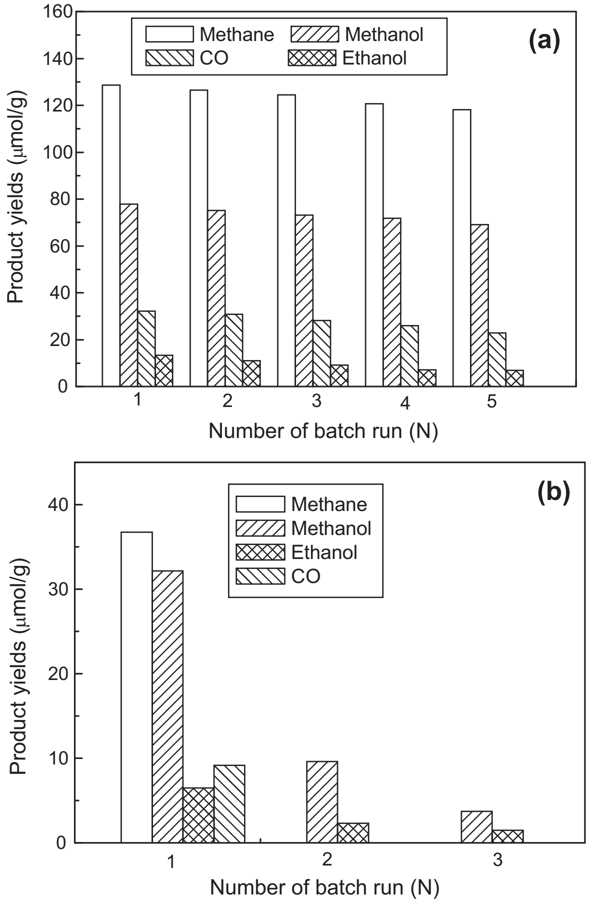

Fig. 9. Yield of photocatalytic products on the number of batch runs for (a) $AgBr/TiO_2$, and (b) AgBr.

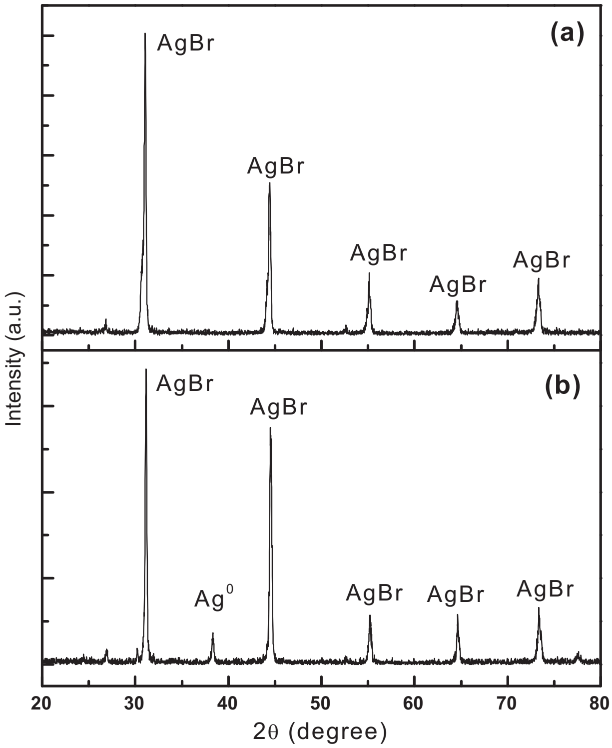

Fig. 10. XRD pattern of (a) fresh AgBr, and (b) used AgBr after visible light irradiation.

3.3. Stability of $AgBr/TiO_2$

For the practical application of such a photocatalytic reduction reaction process, not only the photocatalytic activity of a catalyst is important, but its stability is also critical, since AgBr as a component of $AgBr/TiO_2$ is a photosensitive semiconductor material. Alternatively, both of $AgBr/TiO_2$ and AgBr were tested for their repeated uses and stability for CO_2 photocatalytic reduction in aqueous solution. As shown in Fig. 9a, it can be seen that $AgBr/TiO_2$ retained its yield of methane, methanol, ethanol, and CO in 5 repeated uses at 123.67 ± 4.24, 73.42 ± 3.29, 9.50 ± 2.67 and 28.02 ± 3.73 μmol/g, respectively. The total yields of the photocatalytic products on $AgBr/TiO_2$ after the 5 repeated uses remained about 86% of the first run. The results indicated that $AgBr/TiO_2$ is an effective and chemical-stable catalyst. However, AgBr demonstrated a significant decline of product yield after 3 repeated uses from 36.73 to 0 $\mu mol\,g^{-1}$ for methane, 32.16–3.71 $\mu mol\,g^{-1}$ for methanol, 6.49–1.46 $\mu mol\,g^{-1}$ for ethanol, and 9.18–0 $\mu mol\,g^{-1}$ for CO, respectively (Fig. 9b). The total yields of the photocatalytic products on AgBr after the 3 repeated uses decreased to about 6% of the first run. Furthermore, the used AgBr and $AgBr/TiO_2$ after repeated uses were examined by XRD measurement. Fig. 10 showed the XRD patterns of the fresh and used AgBr. It can be seen clearly that the crystalline Ag can be found in the used AgBr at around $2\theta = 38.2^\circ$ (Fig. 10b) compared to that of fresh AgBr (Fig. 10a), indicating a formation of metallic Ag through the photographic process under visible light irradiation. This result indicated that the decreased activity of pure AgBr is ascribed to the decomposition of the catalyst. However, with respect to $AgBr/TiO_2$, the

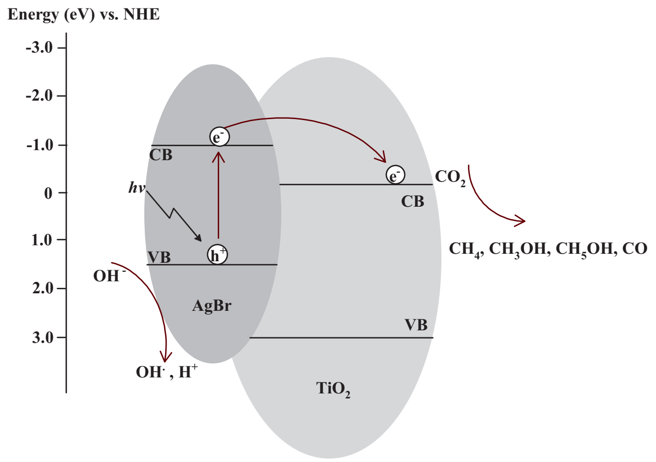

Fig. 11. Schematic of photoexcitation process under visible light.

XRD results show that $AgBr/TiO_2$ after repeated use appeared to display no changes as before (not given here), indicating that AgBr nanoparticles well-dispersed on TiO_2 can maintain their stability and photocatalytic activity. In this photocatalytic process, the transfer of photoexcited electrons from the conduction band of well-dispersed AgBr on catalysts to that of TiO_2 is beneficial for the stability of AgBr [14]. Therefore in practice, the stability of $AgBr/TiO_2$ would be a significant advantage for CO_2 photocatalytic reduction under visible light.

3.4. Photoreduction mechanism of CO_2

The mechanism to account for photo-reduction of CO_2 involves the initial photoexcitation of the catalyst, creating the electron-hole pairs under photoexcitation, followed by their transfer to CO_2 and water [27–29]. For efficient electron transfer between TiO_2 and the semiconductor with narrow band gap, the conduction band of TiO_2 must be more anodic than the corresponding band of the sensitizer. Under visible irradiation, only the semiconductor with narrow band gap is excited, and electrons generated to their conduction band are injected into inactivated TiO_2 conduction band. If the valance band of the sensitizer is more cathodic than the valance band of TiO_2, hole generated in the semiconductor remains there and cannot migrate to TiO_2 [7]. Earlier study reported that the $AgBr/TiO_2$ photocatalyst can be efficiently exited by visible light to generate electron-hole pairs [12–14]. Indeed, the conduction band of AgBr which is located at c.a. −1.04 eV versus NHE is more cathodic than the conduction band of TiO_2 (−0.5 eV) [7,30]. Generally, the higher the difference between conduction bands of two semiconductors, the higher the driving forces of electron injection are [7]. Therefore, under visible light irradiation, only AgBr in $AgBr/TiO_2$ was excited, and the electron in AgBr exited by visible light can transfer from the conduction band of AgBr to that of TiO_2. This process of electron transfer is faster than the electron-hole recombination between the VB and CB of AgBr [30], thus, plenty of CB-electrons (AgBr) can be stored in the conduction band of TiO_2. The absence of metallic Ag in the catalyst after irradiation (Fig. 2c) suggested that interstitial ions failed to capture the photogenerated electrons, which confirmed that the photogenerated electrons in AgBr exited by visible light can transfer to the conduction band of TiO_2. This also can explain the reason why $AgBr/TiO_2$ exhibited higher photocatalytic activity and stability than the pure AgBr for the photoreduction of CO_2. The mechanism of the electron transfer in this system can be illustrated in Fig. 11.

Furthermore, the possible reaction mechanism of CO_2 with H_2O on the catalysts can be proposed in the following way (Eqs. (1)–(10)). The exited holes reacted with adsorbed water molecules on the catalyst surface to form ·OH radicals and H^+ (Eq. (2)) [5,28]. Subsequently, the interaction of H^+ ions with the excited electrons led to ·H radicals (Eq. (3)). Meanwhile, the charge transferred to the conduction band of TiO_2 reacted with CO_2 to form $\cdot CO_2{}^-$ (Eq. (4)) [9,31]. It has been reported that $\cdot CO_2{}^-$ is metastable and factors such as salvation could change the electron affinity of CO_2 [32]. In this case, $\cdot CO_2{}^-$ anion radicals were formed in water with high dielectric constant and can be greatly stabilized by the solvent, resulting in weak interaction of the radical with the catalyst surface [33]. These radicals reacted with each other to produce CO (Eq. (5)) [10,34]. At the same time, carbon radicals (·C) were formed from CO by successive reactions (Eqs. (6)–(7)) [5,29,34], then $\cdot CH_3$ radicals were formed (Eq. (8)) [5,34]. The CH_3 radicals tends to react with protons to produce methane (Eq. (9)) [10,28,33,34], methanol (Eq. (10)) [10,27,28,32]. And ethanol might be converted from methanol at higher CO_2 pressures according to Tseng et al.'s report [27].

$$AgBr/TiO_2 + \text{visible light} \rightarrow e^-(CB) + h^+(VB) \quad (1)$$

$$H_2O + h^+ \rightarrow \cdot OH + H^+ \quad (2)$$

$$H^+ + e^- \rightarrow \cdot H \quad (3)$$

$$CO_2 + e^- \rightarrow \cdot CO_2{}^- \quad (4)$$

$$\cdot CO_2{}^- + \cdot H \rightarrow CO + OH^- \quad (5)$$

$$CO + e^- \rightarrow \cdot CO^- \quad (6)$$

$$\cdot CO^- + H\cdot \rightarrow \cdot C + OH^- \quad (7)$$

$$\cdot C + H^+ + e^- \rightarrow \cdot CH_2 \rightarrow \cdot CH_3 \quad (8)$$

$$\cdot CH_3 + H^+ + e^- \rightarrow CH_4 \quad (9)$$

$$\cdot CH_3 + \cdot OH \rightarrow CH_3OH \quad (10)$$

4. Conclusions

In this contribution, the nanostructured $AgBr/TiO_2$ photocatalyst was prepared by the deposition–precipitation method in the presence of cetyltrimethylammonium bromide (CTAB). The results of characterization showed that AgBr nanoparticles in the $AgBr/TiO_2$ were well dispersed on the surface of TiO_2 nanoparticles and stabilized by the surrounding support of TiO_2. The photocatalytic activities of $AgBr/TiO_2$ photocatalyst was evaluated by the reduction yield in the presence of CO_2 and water under visible light ($\lambda > 420$ nm). The experiment results showed that $AgBr/TiO_2$ with a 23.2% AgBr content had relatively high reduction yields under visible light irradiation. Moreover, it was found that $AgBr/TiO_2$ photocatalyst was stable in the repeated uses under visible light due to the transfer of photoexcited electrons from the conduction band of well-dispersed AgBr to that of TiO_2. This investigation, using $AgBr/TiO_2$ photocatalyst to reduce CO_2 under visible light, will enrich the fundamental theory not only for efficient CO_2 conversion and fixation, storage of solar energy, but also for solving environmental problems.

Acknowledgements

The authors wish to thank the National Natural Science Foundation of China (No. 20877025), the Fundamental Research Funds for the Central Universities (No. 09lgpy20), the Specialized Research Fund for Doctoral Programs of Higher Education from Education Ministry of China (No. 200805611015), Project from Guangzhou City (2010Z2-C1009) and Ministry of Science and Technology of China (No. 10C26214414753), the Research Fund Program of Guangdong Provincial Key Laboratory of Environmental Pollution Control and Remediation Technology (No. 2011K0003), and the

Scientific Research Foundation for the Returned Overseas Chinese Scholars from State Education Ministry for financially supporting this work.

References

[1] D. Luthi, M. Le Floch, B. Bereiter, T. Blunier, J.M. Barnola, U. Siegenthaler, D. Raynaud, J. Jouzel, H. Fischer, K. Kawamura, T.F. Stocker, Nature 453 (2008) 379.
[2] J.E. Dore, R. Lukas, D.W. Sadler, D.M. Karl, Nature 424 (2003) 754.
[3] S.C. Roy, O.K. Varghese, M. Paulose, C.A. Grimes, Acs. Nano 4 (2010) 1259.
[4] P.W. Pan, Y.W. Chen, Catal. Commun. 8 (2007) 1546.
[5] Q.H. Zhang, W.D. Han, Y.J. Hong, J.G. Yu, Catal. Today 148 (2009) 335.
[6] H.W. Slamet, E. Nasution, S. Purnama, J. Kosela, Gunlazuardi, Catal. Commun. 6 (2005) 313.
[7] Y. Bessekhouad, D. Robert, J.V. Weber, J. Photochem. Photobiol. A: Chem. 163 (2004) 569.
[8] P. Usubharatana, D. McMartin, A. Veawab, P. Tontiwachwuthikul, Ind. Eng. Chem. Res. 45 (2006) 2558.
[9] X.H. Xia, Z.H. Jia, Y. Yu, Y. Liang, Z. Wang, L.L. Ma, Carbon 45 (2007) 717.
[10] O.K. Varghese, M. Paulose, T.J. LaTempa, C.A. Grimes, Nano Lett. 9 (2009) 731.
[11] H.C. Liang, X.Z. Li, Appl. Catal. B: Environ. 86 (2009) 8.
[12] C. Hu, Y.Q. Lan, J.H. Qu, X.X. Hu, A.M. Wang, J. Phys. Chem. B 110 (2006) 4066.
[13] M.R. Elahifard, S. Rahimnejad, S. Haghighi, M.R. Gholami, J. Am. Chem. Soc. 129 (2007) 9552.
[14] Y. Zang, R. Farnood, Appl. Catal. B: Environ. 79 (2008) 334.
[15] P.W. Huo, Y.S. Yan, S.T. Li, H.M. Li, W.H. Huang, Desalination 256 (2010) 196.
[16] S. Glaus, G. Calzaferri, Photochem. Photobiol. Sci. 2 (2003) 398.
[17] J. Belloni, M. Treguer, H. Remita, R.D. Keyzer, Nature 402 (1999) 865.
[18] H. Yamada, A.J. Bhattacharyya, J. Maier, Adv. Funct. Mater. 16 (2006) 525.
[19] Y. Yamashita, N. Aoyama, J. Mol. Catal. A 150 (1999) 233.
[20] S. Rodrigues, S. Uma, I.N. Martyanov, K.J. Klabunde, J. Catal. 233 (2005) 405.
[21] C. He, T. Sasaki, Y. Zhou, Y. Shimizu, M. Masuda, N. Koshizaki, Adv. Funct. Mater. 17 (2007) 3554.
[22] Y. Yamashita, N. Aoyama, N. Takezawa, K. Yoshida, Environ. Sci. Technol. 34 (2000) 5211.
[23] Y.Y. Li, Y. Ding, J. Phys. Chem. C 114 (2010) 3175.
[24] F.M. John, F.S. William, in: J. Chastain (Ed.), Handbook of X-ray photoelectron spectroscopy, PerkinElmer Corporation Physical Electronics Division, United States of America, 1992.
[25] V.P. Indrakanti, J.D. Kubicki, H.H. Schobert, Energy Environ. Sci. 2 (2009) 745.
[26] T.V. Nguyen, C.S. Wu, C.H. Chiou, Catal. Commun. 9 (2008) 2073.
[27] I.H. Tseng, W.C. Chang, C.S. Wu, Appl. Catal. B: Environ. 37 (2002) 37.
[28] H. Yamashita, Y. Fujii, Y. Ichihashi, S.G. Zhang, K. Ikeue, D.R. Park, K. Koyano, T. Tatsumi, M. Anpo, Catal. Today 45 (1998) 221.
[29] S.S. Tan, L. Zou, E. Hu, Catal. Today 115 (2006) 269.
[30] L.S. Zhang, K.H. Wong, Z.G. Chen, J.C. Yu, J.C. Zhao, C. Hu, C.Y. Chan, P.K. Wong, Appl. Catal. A 363 (2009) 221.
[31] H. Takeda, O. Ishitani, Coord. Chem. Rev. 254 (2010) 346.
[32] V.P. Indrakanti, H.H. Schobert, J.D. Kubicki, Energy Fuels 23 (2009) 5247.
[33] N. Sasirekha, S.J.S. Basha, K. Shanthi, Appl. Catal. B: Environ. 62 (2006) 169.
[34] K. Koci, L. Obalova, L. Matejova, D. Placha, Z. Lacny, J. Jirkovsky, O. Solcova, Appl. Catal. B: Environ. 89 (2009) 494.